Senescent Changes and Topography of the Dark-Adapted Multifocal Electroretinogram

Panorgias, Athanasios ; Tillman, Megan ; Sutter, Erich E ; Moshiri, Ala ; Gerth-Kahlert, Christina ; Werner, John S

DOI: https://doi.org/10.1167/iovs.16-20953

Senescent Changes and Topography of the Dark-Adapted Multifocal Electroretinogram

Athanasios Panorgias,[1,2] Megan Tillman,[1] Erich E. Sutter,[3] Ala Moshiri,[1] Christina Gerth-Kahlert,[4] and John S. Werner[1,5]

[1]Department of Ophthalmology & Vision Science, University of California Davis Medical Center, Sacramento, California, United States
[2]Department of Vision Science, New England College of Optometry, Boston, Massachusetts, United States
[3]Electro-Diagnostic Imaging, Inc., Redwood City, California, United States
[4]Department of Ophthalmology, University Hospital Zurich, Zurich, Switzerland
[5]Department of Neurobiology, Physiology & Behavior, University of California Davis, Davis, California, United States

Correspondence: Athanasios Panorgias, Department of Vision Science, New England College of Optometry, 424 Beacon Street, Boston, MA 02115, USA; panorgiasa@neco.edu.

Submitted: October 19, 2016
Accepted: January 30, 2017

Citation: Panorgias A, Tillman M, Sutter EE, Moshiri A, Gerth-Kahlert C, Werner JS. Senescent changes and topography of the dark-adapted multifocal electroretinogram. *Invest Ophthalmol Vis Sci*. 2017;58:1323–1329. DOI:10.1167/iovs.16-20953

Purpose. To investigate the topographic changes of the dark-adapted multifocal electroretinogram (mfERG) across adulthood in the central retina and compare the topography between macular versus extramacular, nasal versus temporal, and inferior versus superior retinal areas.

Methods. Sixty-five subjects (18–88 years) received a comprehensive dilated eye examination to ensure the health of their retina and were tested with a dark-adapted mfERG protocol using a 61-hexagon pattern. The lens absorption of each subject was also estimated using a heterochromatic flicker photometry (HFP) paradigm.

Results. The response amplitude and latency of the dark-adapted mfERG showed a significant change with age, which was best described with a linear model. All the retinal areas examined demonstrated similar aging effects. The extramacular and temporal retina showed higher response amplitude and faster response latency when compared with the macular and nasal retinae, respectively. No difference was found in response amplitude and latency between the inferior and superior retina. The HFP results also showed a significant correlation with age, consistent with senescent increases in short wavelength absorption by the crystalline lens. However, the change in lens absorption did not exceed the magnitude of the change in response amplitude and latency.

Discussion. Our results indicate that there is a decline in dark-adapted retinal activity as measured with the mfERG. These aging processes affect rods and rod-bipolar cells. Their decrease in response can be attributed to both optical and neural factors.

Keywords: scotopic vision, mfERG, topography of mfERG, dark-adapted ERG, aging vision

Vision under dark-adapted, or scotopic, conditions is initiated by the rod photoreceptors that reach their maximal sensitivity after approximately 40 minutes in the dark. Many factors determine dark-adapted vision. One such factor is normal aging.[1] Another is pathology, either retinal (i.e., AMD, diabetic retinopathy)[2,3] or systemic (i.e., vitamin A deficiency, Diabetes Mellitus).[4,5] Because the risk of these retinal and systemic pathologies increases with age, compromised dark-adapted vision might be the result of these two factors. Older subjects show a slowing of the dark-adaptation process and they may require up to 90 minutes to reach their maximum sensitivity. Furthermore, older adults also show a reduction in absolute sensitivity, irrespective of the dark-adaptation time.[1] Either way, the common denominator is that the function and kinetics of the rod system are altered. Due to high spatial and temporal summation of the scotopic system, however, detectable changes might not occur after neuronal loss has already taken place.[6] Several studies have also suggested that the rod system is more vulnerable to aging and disease than the cone system,[7,8] making it an 'ideal' candidate for early detection of retinal pathologies.

In vitro photoreceptor topography of excised human retina[8] showed a greater loss of rods in the central 4 mm (~14°) of the retina compared with the periphery. Approximately 34,000 rods are lost per year from early adulthood to the nineties, with the greatest loss occurring between 1 and 2 mm from the fovea. There is, however, reorganization of the remaining rods so that the covered area and rhodopsin density change little throughout adulthood.[8–10] Furthermore, nonuniform rod loss is not reflected by variations in scotopic sensitivity across the retina,[11] suggesting that postreceptoral mechanisms need to be taken into consideration. A suitable test to resolve this discrepancy is the dark-adapted ERG as the origins of its components are post receptoral, namely the b-wave. When the dark-adapted ERG is coupled with the multifocal technique,[12] it offers spatial information that can be used to assess local changes in dark-adapted function. Hood et al.[13] first recorded the dark-adapted multifocal electroretinogram (mfERG) on humans, and Nusinowitz et al.[14] on mice, and later many found useful applications in assessing diseases of the retina.[15–20]

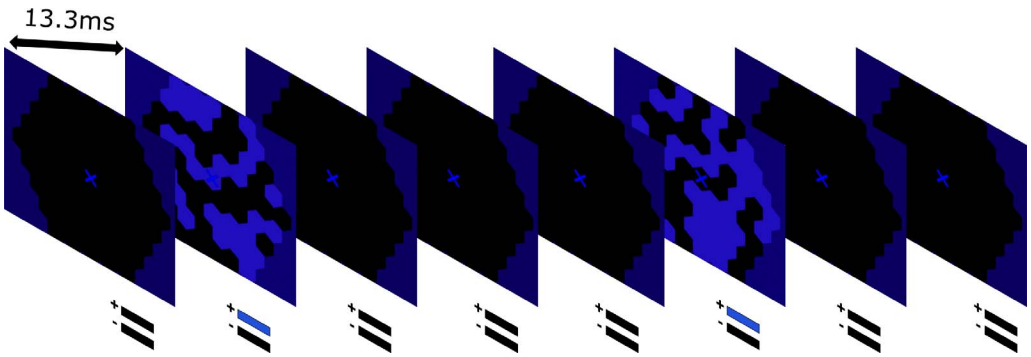

FIGURE 1. The frame sequence used for recording the scotopic mfERGs. The m-sequence started with a blank frame, followed by the stimulus frame and two more blank frames. The stimulator's refresh rate was 75 Hz resulting in a frame duration of 13.3 msec for a total of 66.5-msec interstimulus interval. The figure illustrates 2 m-steps.

None of the aforementioned studies looked into the effect of age on the dark-adapted mfERG, with the exception of Feigl et al.[19] They tested the differences between younger (age range 28–36 years) and older (age range 64–75 years) subject groups. In this study, we sampled across adulthood to obtain objective spatially resolved information about dark-adapted function throughout the central retina (~40°). These results provide normative data for dark-adapted mfERGs throughout adulthood that could be used to detect abnormalities in aging or pathologic conditions.

METHODS

Subjects

Written informed consent was obtained from all subjects. This research followed the tenets of the Declaration of Helsinki and was approved by the University of California Davis' institutional review board. Subjects with systemic pathology known to affect vision (i.e., diabetes) were not included in the study. All subjects underwent a dilated eye exam by an optometrist to rule out any ocular pathology, and monocular LogMAR best-corrected visual acuity (BCVA) was obtained with an Early Treatment Diabetic Retinopathy Study chart. Subjects with BCVA worse than 20/25 and refractive error worse than ± 5.0-diopters (D) sphere and + 2.5-D cylinder were excluded from the study. Color fundus images of 50° without any filters were acquired with a retinal camera (Topcon TRC.501X Retinal Camera; Topcon, Tokyo, Japan). A retinal specialist evaluated the color fundus images, and subjects who were suspected to have any ocular/retinal pathology (i.e., diabetic retinopathy, AMD) were excluded from this study's subject cohort. Sixty-five subjects (age range 18–88 years) participated. All were classified as AREDS category I (fewer than 5 small drusen [<63 μm], and BCVA of 20/32 or better in both eyes).[21] There were approximately 10 subjects per each age decade starting at 18 years.

Scotopic mfERGs

Scotopic mfERGs were recorded from one eye of each subject; whichever had the highest BCVA. The Veris Pro 6.3.2 was used with the FMS III stimulator running at 75 Hz (EDI, Redwood City, CA, USA). The pupil was dilated with 1% tropicamide and 2.5% phenylephrine. Our lab found that this combination of tropicamide and phenylephrine ensures maximum dilation for both the younger and older observers with no significant group differences in the diameter of the dilated pupil.[22] Multifocal electroretinogram responses were obtained using a DTL electrode (Diagnosys LLC, Lowell, MA, USA) and standard ground and reference gold-cup electrodes, which were placed on the forehead and close to the temporal canthus, respectively, according to International Society for Clinical Electrophysiology of Vision standards for photopic mfERGs.[23] The impedance was measured with VERIS' built-in feature and maintained below 5 KΩ for the entirety of the procedure. A 1°

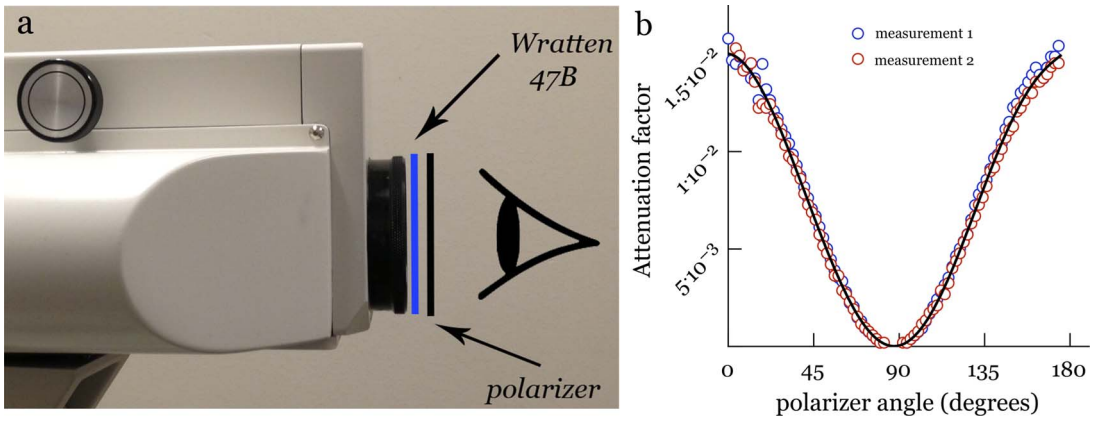

FIGURE 2. (a) The FMS III configuration with the Wratten 47B filter and the linear polarizer. The polarizer was mounted on a ring attached to the eyepiece of the FMS III. Marks on the FMS III and a linear scale attached to the rim of the polarizer ring allowed accurate rotation of the polarizer and the same polarization angle for each subject. (b) The luminance attenuation factor as a function of the polarizer's angle. We measured the luminance attenuation factor twice to ensure reproducibility of the desired experimental luminance. The solid curve is the best-fitted sinusoidal function.

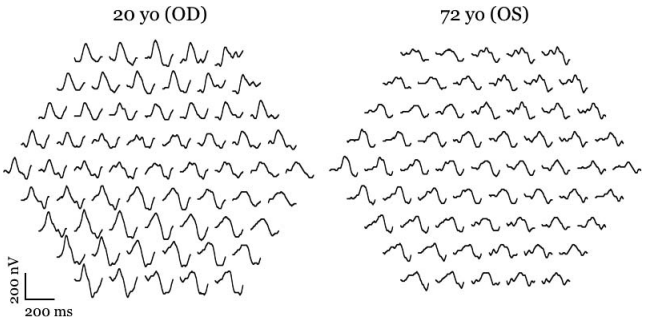

FIGURE 3. The dark-adapted mfERG traces for two observers, a 20-year-old on the *left* and a 72-year-old on the *right*. Note the differences in amplitude and timing between the two subjects for the majority of the localized responses.

cross in the central hexagon was used as a fixation target. During each recording segment, the fixation target blinked 3 to 10 times and the subjects were instructed to count the blinks and report the number at the end of the recording. This task was challenging for subjects of all ages, but it was effective for maintaining alertness and fixation.

Scotopic mfERG responses were recorded after a 40-minute period of dark adaptation. The dark-adapted mfERG protocol is described elsewhere.[20] Briefly, an unscaled 61-hexagonal pattern was used to elicit the responses from the central approximately 40°, resulting in a resolution of approximately 4.4° per hexagon. An m-sequence of 14 resulted in approximately 14-minutes recording time that was split into approximately 30-second segments. Inserting three blank frames (one before the stimulus and two after, Fig. 1) slowed the m-sequence.[13] The blank frame at the beginning of the sequence was inserted to avoid any possible rod adaptation prior to the beginning of the recordings. This configuration resulted in four frames per m-step with three blank frames in between the stimulus frames. We should acknowledge the fact that reducing the number of frames in the m-sequence results in reduced rod response as discussed in Hood et al.[13] However, this should not be a reason for concern, as long as future recordings that are compared with the present recordings follow the same recording protocol. The amplifier gain was 100 K, the signal was sampled at 4800 Hz, and the low- and high-frequency cut-offs were set to 3 and 100 Hz, respectively, with the ability for offline filtering.

The blue LED of the system (λ_{max} ~450 nm) was used to shape the spectral output of the stimulator. A linear polarizer and a Kodak Wratten-47B filter (dominant $\lambda = 466$ nm) were placed in front of the stimulator to produce scotopic luminances (Fig. 2a) with short wavelength spectral characteristics. The luminance of the stimulator was calibrated for different polarization angles with a photometer (Minolta ChromaMeter; Konica Minolta, Tokyo, Japan; Fig. 2b).

The VERIS infrared camera that captures the subject's eye or fundus during recordings was not able to operate when the radiant power of the infrared light emitting diodes (LEDs) was reduced with the use of a neutral density filter to scotopic levels. The stimulator and the infrared camera, however, are placed on different optical paths within the FMS III, the one containing a linear polarizer (stimulator) and the other not (infrared camera). This configuration allowed us to control the luminance of the stimulator with an external linear polarizer while the optical path of the infrared camera remained unaffected, thereby permitting visualization of the subjects' eye during scotopic recordings. The luminance of the bright state was −2.5 log cd/m^2 and that of the dark state close to zero resulting in more than 99% contrast. The surrounding background luminance was set to −2.8 log cd/m^2 so as to minimize the stray light effects, as discussed in Hood et al.[13]

The amplitude of the dark-adapted mfERG was measured from the baseline to the peak of the response. According to the photopic mfERG nomenclature, this peak corresponds to the P1.[24] Similarly, the response latency was measured from the onset of the stimulus to the peak.

Heterochromatic Flicker Photometry

Heterochromatic flicker photometry was used to estimate the relative optical density of each subject's ocular media. The blue and red phosphors of a CRT monitor (FlexScan; EIZO, Hakusan, Japan) were flickered in 20-Hz sinusoidal counterphase. The two lights formed an annular disk of approximately10° to 40° inner/outer diameter using a ViSaGe graphics card and the Visual Psychophysics Engine (Cambridge Research Systems Ltd, Rochester, UK). The central 10° of the stimulus was removed to avoid confounding effects of macular pigment absorption. The luminances of the two disks were yolked so that the sum of the red and blue phosphor luminance was always 30 cd/m^2. The task for the subjects was to change the relative luminance of the two disks so as to minimize the perceived flicker. For example, if the subject set the ratio R/(R+B) (where R is the luminance of the red phosphor and B is the luminance of the blue phosphor) at 0.5, then R=B, the point of minimum flicker. A lower ratio means that the ocular media of this subject absorbed more short-wavelength light; greater short-wave radiance was required for equiluminance. Knowing that the lens absorbs mainly at short

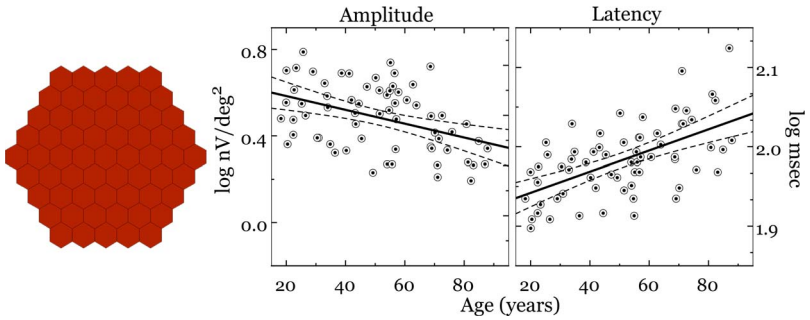

FIGURE 4. Amplitude and latency of the averaged approximately 40° dark-adapted mfERGs as a function of age. The *left-most panel* shows the grouping of the hexagons for the results reported in this figure. The *middle panel* shows the log nV/deg^2 of the averaged responses as a function of age. The *right panel* shows the log latency of the dark-adapted mfERG responses as a function of age. The *solid lines* are linear regressions, and the *dashed lines* are 95% confidence bounds for the linear fit. For amplitude, the slope of the linear regression is –0.0032 nV/deg^2/year ($r = -0.4172$, $P < 0.01$). For latency, the slope of the linear regression is 0.0013 log ms/year ($r = 0.5744$, $P < 0.001$).

Table 1. Slopes of Amplitude and Latency for Each Retinal Area

mfERG Component	Whole	Macular	Extramacular	Nasal	Temporal	Superior	Inferior
Amplitude, log nV/deg^2/year	−0.0032	−0.003	−0.00269	−0.00239	−0.0030	−0.00203	−0.00237
Latency, log msec/year	0.0013	0.00123	0.00128	0.00127	0.00122	0.00162	0.00114

wavelengths and its optical density increases with age, we would expect that the R/(R+B) would decrease as a function of age.

Results

Figure 3 shows the scotopic mfERGs of two subjects ages 20- and 72-years old. Note that both subjects show a slight reduction in the amplitude of the dark-adapted mfERGs in the central retinal areas.

To study changes in the dark-adapted mfERG with age, and be able to compare it with histologic studies, we grouped the traces of the 61 hexagons in four different configurations. Figure 4 shows the results of the first analysis. All responses from the stimulated retinal area were averaged to quantify the aging effect throughout approximately 40° of the central retina. The left panel shows the grouped hexagons (i.e., the whole retinal area). The two other panels show the amplitude (middle) and latency (right) of the dark-adapted mfERGs as a function of age. There is a significant negative correlation between log amplitude and age ($r = –0.4172$, $P < 0.01$) as well as a significant positive correlation between log latency and age ($r = 0.5744$, $P < 0.001$). Amplitude decreased by 0.0032 log nV/deg^2/year and latency increased by 0.0013 log msec/year (see Table 1 for a summary of the slope values).

The second hexagon grouping is shown in Figure 5 to separate responses from the central 20° of the retina (called the macular area) and a 10° ring subtending 10° to 20° eccentricity (called the extramacular area), as shown in the left panel of Figure 5. The extramacular area shows higher amplitude and faster latency compared with the responses of the macular area (see Table 2 for P values for testing the differences in amplitude and latency between the paired retinal locations).

There is a significant correlation between amplitude and age and between latencies and age for both areas. The amplitude of the extramacular area declined by 0.00269 log nV/deg^2/year ($r = –0.3230$, $P < 0.05$) and that of the macular area by 0.0030 log nV/deg^2 ($r = –0.3278$, $P < 0.05$). The latency of the extramacular area increased by 0.00128 log msec/year ($r = 0.5579$, $P < 0.005$) and that of the macular area by 0.00123 log msec/year ($r = 0.5255$, $P < 0.01$). There was no significant interaction between the two areas and age for slopes of amplitude ($P = 0.8307$) or latency ($P = 0.8864$).

The third analysis, shown in Figure 6, separates the nasal and temporal retina. Each area subtends approximately 20° of retinal eccentricity as shown in the left panel of Figure 6. The temporal retina shows a significantly higher amplitude and faster latency compared with the nasal retina (Table 1). There is a significant correlation between amplitude and age and latency and age for both the temporal and nasal retina. The amplitude of the temporal retina decreased by 0.0030 nV/deg^2/year ($r = –0.3399$, $P < 0.01$) and that of the nasal retina by 0.00239 nV/deg^2/year ($r = –0.2958$, $P < 0.05$). The latency of the temporal retina increased by 0.00122 log msec/year ($r = 0.5595$, $P < 0.001$) and that of the nasal retina by 0.00127 log msec/year ($r = 0.5171$, $P < 0.001$). Testing for interactions between the two areas and age shows that there is no statistically significant difference between the slopes of amplitude ($P = 0.0.6744$) or latency ($P = 0.8828$) for the two retinal areas.

The final hexagon configuration, shown in Figure 7, separates the responses from the superior and inferior retina. Each area subtends approximately 20° of retinal eccentricity. There is no statistically significant difference between the amplitudes of the two retinal areas, but there is a significant difference between their latencies (Table 1). There is a significant correlation between amplitude and age and latency and age for both the superior and inferior retina. The amplitude of the superior retina decreases by 0.00203 nV/deg^2/year ($r = –0.2545$, $P < 0.05$) and that of the inferior retina by 0.00237 nV/deg^2/year ($r = –0.2987$, $P < 0.05$). The latency of the superior retina increases by 0.00162 log msec/year ($r = 0.6279$, $P < 0.001$) and that of the inferior retina by 0.00114 log msec/year ($r = 0.4862$, $P < 0.001$). There was no significant interaction between the two retinal areas and age for either slopes of amplitude ($P = 0.8051$) or latency ($P = 0.1836$).

Figure 8 shows the results of the HFP experiment. There is a significant correlation between HFP and age ($r = –0.591$, $P < 0.001$). The HFP ratio is higher for younger observers and

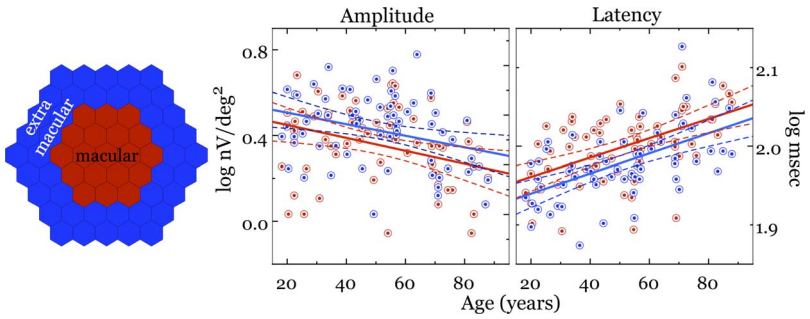

Figure 5. Mean amplitude and latency for two retinal areas. The macular area of approximately 20° diameter and the extramacular area forming a ring of approximately 10° diameter between 10° and 20° retinal eccentricity (*left panel*). The *middle* and *right panels* show the log nV/deg^2 and log ms of the averaged responses as a function of age. *Red data points* and *fitted lines* correspond to the macular area; *blue data points* and *fitted lines* correspond to the extramacular area. The *dashed lines* are the 95% confidence bounds for the linear regressions. For the macular area, the amplitude slope is –0.003 nV/deg^2/year ($r = –0.3278$, $P < 0.05$) and the latency slope is 0.00123 log ms/year ($r = 0.5255$, $P < 0.01$). For the extramacular area, the amplitude slope is –0.00269 nV/deg^2/year ($r = –0.3230$. $P < 0.05$) and the latency slope is 0.00128 log ms/year ($r = 0.5579$, $P < 0.005$).

Table 2. *P* Values for Differences in Amplitude and Latency (Paired-Sample, Two-Tail *t*-Test) Between the Paired Retinal Locations in Figures 5, 6, and 7

	P Values for Differences	
Retinal Area	**Amplitude**	**Latency**
Macular vs. extramacular	0.0219	0.0045
Nasal vs. temporal	0.0365	0.0102
Superior vs. inferior	0.4804	0.0851

lower for older observers, indicating that the older observers require more short-wave light to equate the luminances of the red and blue phosphors. This increase is proportional to the higher optical density of the lens in older individuals.

Discussion

This study describes rod-mediated function as measured with the dark-adapted mfERG. In general, there is a significant negative correlation between age and amplitude as well as a significant positive correlation between age and response latency. The current study also examined the topography of the dark-adapted mfERG. Statistically significant differences in amplitude and latency were found between nasal and temporal retina and between the macular and extramacular areas. No significant difference was found between inferior and superior retina. No statistically significant difference was found in the amplitude and latency slopes for the three paired locations examined here, meaning that no retinal area was found to be more vulnerable to normal age-related change with the mfERG. In the current study, we also estimated the relative degree of short-wavelength absorbance by the aging ocular media using an HFP paradigm so as to disentangle the neural losses from those due to reduced retinal illuminance in the aging eye. A significant negative correlation between age and the HFP ratio was found as expected, suggesting an increased absorbance of short-wavelength light by the ocular media of the older adults. When comparing the results between the dark-adapted mfERGs and HFP experiments, the slopes in the mfERG response amplitude were greater, in general, than that of the HFP ratio. Therefore, the difference between the slopes of response amplitude and HFP slope can be at least partly attributed to senescent retinal mechanisms and not optical factors alone.

As already mentioned, this study fills a gap in the literature regarding the aging of the mfERG responses throughout adulthood. A previous study by Feigl et al.[19] examined age-related change in the dark-adapted mfERG response between a small cohort of younger ($n = 10$, 28–36 years) and older adults ($n = 10$, 64–75 years). Feigl et al.[19] did not find a difference in amplitude between the two age groups. Given the variability of the response amplitude in our study, a small number of participants might not be sufficient to reveal any age-related differences. However, the authors[17] did find a significant delay in the older adults' response latency. The variability in response latency is, in general, much lower than that of the amplitude variability (~0.2 log units compared with ~0.8 log units for the response amplitude in our study), which could explain the discrepancy in amplitude differences between the two studies. Also, we recruited a broader age range with approximately 10 subjects per decade, which allowed us to examine changes in the dark-adapted mfERG across adulthood.

Our results are not directly comparable with those obtained with full-field dark-adapted ERGs due to differences in rod population and neural sampling in the extreme peripheral retina. Nevertheless, it is worth noting that Birch et al.[25] found an age-related decline in full-field dark-adapted ERG amplitude in a cohort of subjects with ages ranging between 1 week and 79 years, with the vast majority of their subjects being between 5 and 25 years. Our results are consistent with their results, even if they can be only qualitatively compared, as both studies agree that there is a decline in the dark-adapted response amplitude with age.

The decrease in response amplitude and increase in response latency in the dark-adapted mfERG could be attributed to several factors. One factor is the difference in the spectral composition of the retinal image across the different ages. The higher absorption of short-wavelength light by the aging ocular media means that the retinal illuminance is reduced in older adults at the area of the visible spectrum where the rods are most sensitive. Age-adjusted corrections could be made for the retinal illuminance following lens absorption models,[6,26,27] but in this study, we directly estimated the relative density of the ocular media based on HFP. The difference between the amplitude versus age slopes and the HFP ratio versus age slope shows that the lens absorption indeed is a factor contributing to the age-dependent reduction in response. However, increased lens absorption cannot completely explain the loss in the dark-adapted mfERG signal in the older adults.

Additional factors that may have contributed to our results could be age-related rod apoptosis as well as changes in the permeability of the RPE/Bruch's membrane complex. Curcio et al.[8] showed that the number of rods significantly decreased within a 6-mm radius from the center of the retina (~20°) as a function of age. The peak dropout was found at approximately

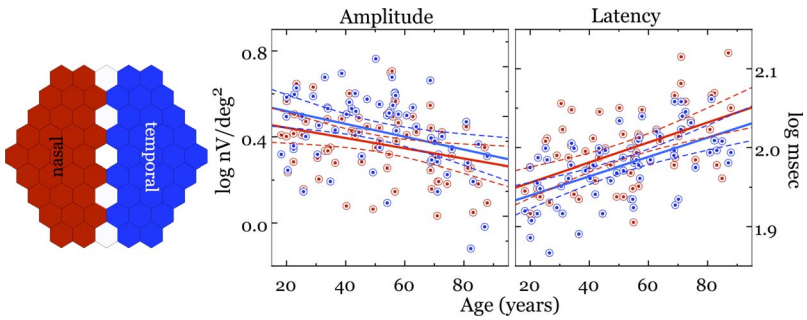

Figure 6. Amplitude and latency of averaged responses for two retinal areas; the nasal retina (*red*) and the temporal retina (*blue*). See Figure 5 legend for details. Both areas subtend approximately 20°. The *middle panel* shows the log nV/deg² as a function of age and the *right panel* the log latency as a function of age for both retinal areas. For the nasal retina, the amplitude slope is –0.00239 nV/deg²/year ($r = -0.2958$, $P < 0.05$) and the latency slope is 0.00127 log ms/year ($r = 0.5171$, $P < 0.001$). For the temporal retina, the amplitude slope is –0.0030 nV/deg²/year ($r = -0.3399$, $P < 0.01$) and the latency slope is 0.00122 log ms/year ($r = 0.5595$, $P < 0.001$).

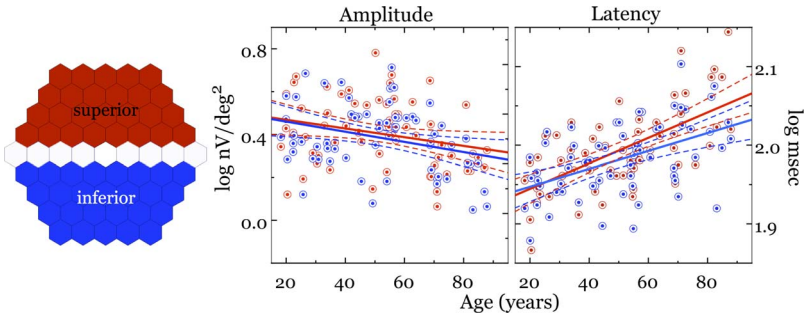

Figure 7. Amplitude and latency of averaged responses for the superior retina (*red*) and inferior retina (*blue*). See Figure 5 legend for details. Both areas subtend approximately 20°. The *middle panel* shows the log nV/deg^2 as a function of age and the *right panel* the log latency as a function of age for both retinal areas. For the superior retina, the amplitude slope is −0.00203 nV/deg^2/year ($r = -0.2545$, $P < 0.05$) and the latency slope is 0.00162 log ms/year ($r = 0.6279$, $P < 0.001$). For the inferior retina, the amplitude slope is −0.00237 nV/deg^2/year ($r = -0.2987$, $P < 0.05$) and the latency slope is 0.00114 log ms/year ($r = 0.4863$, $P < 0.001$).

2-mm eccentricity (~7°) while the rate of rod death is approximately 340,000 rods/year in the central 4-mm eccentricity (~13°). Experiments that estimate rod kinetics (namely the slope of the rod-phase in dark adaptation measurements) also point to changes in the rhodopsin regeneration rate with age.[1,2] Older adults show slower rates of dark adaptation when compared with younger adults. One possible explanation might be that the RPE/Bruch's membrane complex that facilitates nutrient transport from the choriocapillaris to the photoreceptors becomes less efficient over time.[1,7] The transport of nutrients necessary for the retinoid cycle, such as vitamin A through the RPE/Bruch's membrane complex might be obstructed in older adults and alter the rod-response. Of course, we need to acknowledge that dark adaptation responses are much more complex in nature than the responses we describe in this study, as they potentially involve mechanisms beyond the rods and bipolar cells that mediate dark-adapted ERG responses.

In addition to the overall age-related changes, we examined the variation in scotopic mfERG responses between several retinal areas. A significant difference in response amplitude and latency was found between the macular and extramacular areas, with the larger amplitude and faster response latency in the extramacular area. These findings can probably be explained by the rod distribution and rod convergence across the retina. The peak rod density appears at approximately 20° eccentricity, an area that falls in the extramacular group in our configuration, and could explain the elevated P1 amplitude. Similarly, increased rod convergence to bipolar cells in the peripheral retina, might mean faster bipolar cell latency due to the sum of many more rod responses converging onto a single bipolar cell. This would be consistent with psychophysical

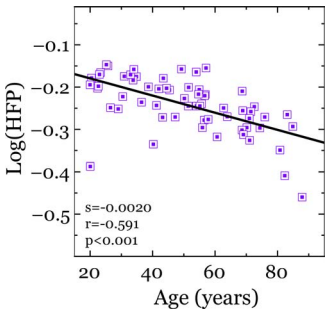

Figure 8. The results of the HFP experiment as a function of age. The line is the best-fitted linear regression. The slope of the regression line is −0.0020 ($r = -0.591$, $P < 0.001$).

results of Arden and Weale[28] demonstrating faster dark adaptation rates with larger stimuli.

Nasal-temporal asymmetries in the retina are well documented in various studies that involve primarily cone sensitivity[29,30] but also rod sensitivity,[31] and they all point to the temporal visual field (nasal retina) exhibiting better performance. Between the nasal and temporal retina, rod density is slightly higher in the nasal retina, especially in the periphery, however, the presence of the optic disk creates a drop in the rod density and consequently in rod sensitivity at this area. The average area of the optic disk is roughly 10 mm^2, while the area of the nasal retina that has been stimulated in our experiments is approximately 54 mm^2. Hence, the optic disk occupies 20% of the nasal retina, which could explain the lower response amplitude we found in this study. The density of the rods is similar between the superior and inferior retina, thus reflecting the similar response amplitudes between the two regions found here.

The findings of the present study demonstrate the localized changes in the rod-mediated activity of the central retina that occur during adulthood and provide reference data for studies of retinal and macular diseases. Although normal aging appears to affect the dark-adapted mfERG responses similarly across retinal locations, as we have shown earlier,[20] the mfERG has the power to detect localized changes in retinal function in ocular pathologies that manifest themselves in particular regions of the retina (i.e., AMD). Moreover, the spatial resolution of the scotopic mfERG has an advantage over psychophysical methods for revealing retinal abnormalities that might be masked by downstream visual processes.

Acknowledgments

The authors thank S.M. Garcia for subject recruitment, coordination, and testing.

Supported by National Institutes of Health Grants AG04058 and EY014743 (Bethesda, MD, USA).

Disclosure: **A. Panorgias**, None; **M. Tillman**, None; **E.E. Sutter**, Electro-Diagnostic Imaging, Inc. (I, E, C, R), P; **A. Moshiri**, None; **C. Gerth-Kahlert**, None; **J.S. Werner**, None

References

1. Jackson GR, Owsley C, McGwin G Jr. Aging and dark adaptation. *Vision Res*. 1999;39:3975–3982.
2. Owsley C, Jackson GR, White M, Feist R, Edwards D. Delays in rod-mediated dark adaptation in early age-related maculopathy. *Ophthalmology*. 2001;108:1196–1202.

3. Bavinger JC, Dunbar GE, Stem MS, et al. The effects of diabetic retinopathy and pan-retinal photocoagulation on photoreceptor cell function as assessed by dark adaptometry. *Invest Ophthalmol Vis Sci*. 2016;57:208–217.
4. Hecht S, Mandelbaum J. The relation between vitamin A and dark adaptation. *JAMA*. 1939;112:1910–1916.
5. Henson DB, North RV. Dark adaptation in diabetes mellitus. *Br J Ophthalmol*. 1979;63:539–541.
6. Tillman MA, Panorgias A, Werner JS. Age-related change in fast adaptation mechanisms measured with the scotopic full-field ERG. *Doc Ophthalmol*. 2016;132:201–212.
7. Curcio CA, Owsley C, Jackson GR. Spare the rods, save the cones in aging and age-related maculopathy. *Invest Ophthalmol Vis Sci*. 2000;41:2015–2018.
8. Curcio CA, Millican CL, Allen KA, Kalina RE. Aging of the human photoreceptor mosaic: evidence for selective vulnerability of rods in central retina. *Invest Ophthalmol Vis Sci*. 1993;34:3278–3296.
9. Plantner JJ, Barbour HL, Kean EL. The rhodopsin content of the human eye. *Curr Eye Res*. 1988;7:1125–1129.
10. Liem AT, Keunen JE, van Norren D, van de Kraats J. Rod densitometry in the aging human eye. *Invest Ophthalmol Vis Sci*. 1991;32:2676–2682.
11. Jackson GR, Owsley C, Cordle EP, Finley CD. Aging and scotopic sensitivity. *Vision Res*. 1998;38:3655–3662.
12. Sutter EE, Tran D. The field topography of ERG components in man—I. The photopic luminance response. *Vision Res*. 1992/3;32:433–446.
13. Hood DC, Wladis EJ, Shady S, Holopigian K, Li J, Seiple W. Multifocal rod electroretinograms. *Invest Ophthalmol Vis Sci*. 1998;39:1152–1162.
14. Nusinowitz S, Ridder WH III, Heckenlively JR. Rod multifocal electroretinograms in mice. *Invest Ophthalmol Vis Sci*. 1999;40:2848–2858.
15. Holopigian K, Shuwairi SM, Greenstein VC, et al. Multifocal visual evoked potentials to cone specific stimuli in patients with retinitis pigmentosa. *Vision Res*. 2005;45:3244–3252.
16. Holopigian K, Seiple W, Greenstein VC, Hood DC. Multifocal cone and rod responses in patients with progressive cone dystrophy. Presented at the 38th Symposium of the International Society for Clinical Electrophysiology of Vision, February 16, 2000; Sydney, Australia.
17. Holopigian K, Seiple W, Greenstein VC, Hood DC, Carr RE. Local cone and rod system function in progressive cone dystrophy. *Invest Ophthalmol Vis Sci*. 2002;43:2364–2373.
18. Feigl B, Brown B, Lovie-Kitchin J, Swann P. Cone- and rod-mediated multifocal electroretinogram in early age-related maculopathy. *Eye*. 2005;19:431–441.
19. Feigl B, Brown B, Lovie-Kitchin J, Swann P. The rod-mediated multifocal electroretinogram in aging and in early age-related maculopathy. *Curr Eye Res*. 2006;31:635–644.
20. Panorgias A, Zawadzki RJ, Capps AG, Hunter AA, Morse LS, Werner JS. Multimodal assessment of microscopic morphology and retinal function in patients with geographic atrophy. *Invest Ophthalmol Vis Sci*. 2013;54:4372–4384.
21. Age-Related Eye Disease Study Research Group. A randomized, placebo-controlled, clinical trial of high-dose supplementation with vitamins C and E, beta carotene, and zinc for age-related macular degeneration and vision loss: AREDS report no. 8. *Arch Ophthalmol*. 2001;119:1417–1436.
22. Gerth C, Sutter EE, Werner JS. mfERG response dynamics of the aging retina. *Invest Ophthalmol Vis Sci*. 2003;44:4443–4450.
23. Hood DC, Bach M, Brigell M, et al. ISCEV standard for clinical multifocal electroretinography (mfERG) (2011 edition). *Doc Ophthalmol*. 2012;124:1–13.
24. Hood DC, Frishman LJ, Saszik S, Viswanathan S. Retinal origins of the primate multifocal ERG: implications for the human response. *Invest Ophthalmol Vis Sci*. 2002;43:1673–1685.
25. Birch DG, Anderson JL. Standardized full-field electroretinography. Normal values and their variation with age. *Arch Ophthalmol*. 1992;110:1571–1576.
26. Pokorny J, Smith VC, Lutze M. Aging of the human lens. *Appl Opt*. 1987;26:1437–1440.
27. Van De Kraats J, Van Norren D. Optical density of the aging human ocular media in the visible and the UV. *JOSA A*. 2007;24:1842–1857. Available at: https://www.osapublishing.org/abstract.cfm?uri=josaa-24-7-1842. Accessed September 13, 2016.
28. Arden GB, Weale RA. Nervous mechanisms and dark-adaptation. *J Physiol*. 1954;125:417–426.
29. Panorgias A, Parry N, McKeefry DJ. Nasal-temporal differences in cone-opponency in the near peripheral retina. *Ophthalmic Physiol Opt*. 2009;29:375–381.
30. Díez-Ajenjo MA, Capilla P, Luque MJ. Red-green vs. blue-yellow spatio-temporal contrast sensitivity across the visual field. *J Mod Opt*. 2011;58:1736–1748.
31. Allen D, Hess RF, Nordby K. Is the rod visual field temporally homogeneous? *Vision Res*. 1998;38:3927–3931.

Investigative Ophthalmology & Visual Science